



## Short Communication

Volume 3 Issue 4 - December 2017  
DOI: 10.19080/JOJMS.2017.03.555617

JOJ Material Sci

Copyright © All rights are reserved by Aleksey A Vedyagin

# Synthesis of Nanocrystalline Oxide Ceramic Materials: a Carbon Nanoreactor Concept



Alexander M. Volodin, Alexander F. Bedilo, Aleksey A. Vedyagin\* and Vladimir O. Stoyanovskii

Boreskov Institute of Catalysis SB RAS, Novosibirsk, Russia

Submitted: December 06, 2017; Published: December 15, 2017

\*Corresponding author: Aleksey A Vedyagin, Boreskov Institute of Catalysis SB RAS, Novosibirsk, Russia, Email: [vedyagin@catalysis.ru](mailto:vedyagin@catalysis.ru)

## Abstract

Carbon-coated nanocrystalline oxides  $\text{TiO}_2@\text{C}$ ,  $\text{Al}_2\text{O}_3@\text{C}$  and calcium aluminate C12A7@C were synthesized, and the effect of carbon coating on their thermal stability and reactivity was studied. It was found that the carbon coating prevents sintering of the titanium nanoparticles and contributes to stabilization of their size. Thus, the particle size of anatase can be stabilized at level of 10-12 nm even after heat treatment at 750°C. Deposition of the carbon coating on  $\gamma\text{-Al}_2\text{O}_3$  prevents growth of the alumina nanoparticles and substantially improves their thermal stability. Complete  $\text{Al}_2\text{O}_3$  conversion to corundum occurs after heat treatment at 1250°C, whereas practically no corundum is formed under similar conditions for  $\text{Al}_2\text{O}_3@\text{C}$ . Dispersed calcium aluminate C12A7 particles resistant to sintering at high-temperature were synthesized inside the carbon shell. Meanwhile, intense sintering at high temperatures was observed for the samples without the carbon coating. The carbon shell prevents sintering and makes it possible to synthesize samples in a disperse state even at 1450°C. According to TEM data, characteristic sizes of C12A7 particles inside the carbon coating range from 100 nm to several microns. So, the core-shell approach can be used to stabilize the size of the oxide core nanoparticles up to temperatures when their reaction with the coating material occurs. In the case of the carbon shell, this is the temperature when the carbothermal reduction of the oxide core takes place.

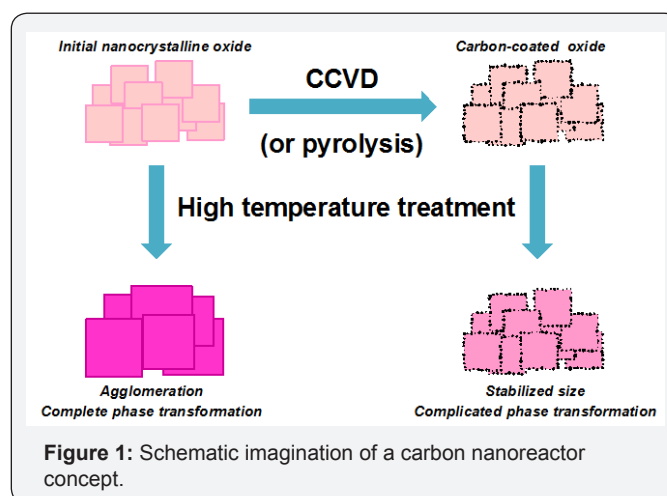
**Keywords:** Nanocrystalline oxides; Carbon nanoreactor; Titanium; Alumina; Calcium aluminate; Phase transformation

## Introduction

Size effects play an important role in various chemical and phase transformations of oxides. For example, nanocrystalline mesoporous oxides often have high reactivity in many chemical reactions making them efficient catalysts [1,2] and destructive sorbents [3-7] for neutralization of various toxic compounds. However, products resulting from their solid-state reactions are usually non-nanocrystalline. Solid-state reactions of nanocrystalline oxides are typically accompanied by particle sintering and formation of a new phase in the form of significantly enlarged particles. The same is true for the phase transformations taking place with the temperature increase and leading to the growth of the precursor nanoparticles.

Unique properties of calcium aluminate with  $12\text{CaO} \cdot 7\text{Al}_2\text{O}_3$  stoichiometric often labeled as C12A7 were discovered and investigated in numerous studies by Hosono et. al [8-10]. These materials contain a stable cation framework  $[\text{Ca}_{24}\text{Al}_{28}\text{O}_{64}]^{4+}$  and changeable anion sub lattice  $4\text{X}^-$ . Chemical and physical properties of these materials can be varied in a wide range by varying the  $\text{X}^-$  anions, where  $\text{X}^-$  can be  $\text{H}^-$ ,  $\text{O}^-$ ,  $\text{O}_2^-$ ,  $\text{O}^{2-}$ ,  $\text{OH}^-$ ,  $\text{Cl}^-$ ,  $\text{F}^-$ ,  $\text{e}^-$ . Recently we have demonstrated that the carbon coating deposited on the surface of oxide nanoparticles can act as a nanoreactor shell. The schematic imagination of the carbon nanoreactor concept is shown in Figure 1. The carbon coating prevents sintering of nanoparticles inside the shell during at high temperatures and stabilizes their size. Moreover, such coating can

be penetrable for reactant molecules from both the gas or liquid phases [7,11-13] making it possible to initiate various catalytic or solid-state reactions inside the nanoreactor. This study is devoted to investigation of phase and chemical transformations of carbon-coated nanocrystalline oxides  $\text{TiO}_2@\text{C}$ ,  $\text{Al}_2\text{O}_3@\text{C}$  and calcium aluminate C12A7@C.



## Experimental

Nanocrystalline  $\text{TiO}_2$  hereinafter abbreviated as NA- $\text{TiO}_2$  was obtained by a sol-gel method using titanium n-but oxide as a

precursor and a mixture of ethanol and toluene with a volume ratio of 1:3 as a solvent. Nitric acid was added to the solution in a ratio of 0.1mol per 1mol of Ti. Then it was hydrolyzed by a stoichiometric amount of water at a room temperature. The resulting white gel was dried in an oven at 110°C for 1 day. The specific surface area SSA of the dried sample with amorphous structure was 540m<sup>2</sup>/g. After calcination in air at 500 °C, the SSA of the sample was about 90m<sup>2</sup>/g.  $\gamma$ -Al<sub>2</sub>O<sub>3</sub> sample used as a precursor for synthesis of all other samples was obtained by calcination of Condea "Pural SB-1" pseudoboehmite sample in air at 720 °C for 6 h with prior temperature increase to 720 °C at a ramping rate of 1.5 °C/min. The SSA of this sample was about 210m<sup>2</sup>/g. In order to prepare the carbon shell, the  $\gamma$ -Al<sub>2</sub>O<sub>3</sub> and TiO<sub>2</sub> precursors were mixed with polyvinyl alcohol PVA in a 7:3 weight ratio. Then, the obtained mixture was heated in a quartz reactor in an argon flow to 750°C with 1.5°C/min heating rate and kept at this temperature for 6 h for  $\gamma$ -Al<sub>2</sub>O<sub>3</sub> and 3 h for TiO<sub>2</sub>. For treatment at higher temperatures, the obtained sample was placed into a graphite crucible that was installed into a corundum tube assembled inside a tubular Star bar TSR heater. Then the sample was heated in an argon flow with the heating rate of 3 °C/min up to the desired temperature varied from 960 to 1450°C and kept at this temperature for 6 h. A mixture of aluminum and calcium hydroxides of required stoichiometric was used as a precursor for C12A7 synthesis. The mixture was thoroughly stirred in distilled water for 10h, filtered, dried at 110°C and calcined at 550°C for 6h.

The obtained C12A7-550 sample was used as a precursor for further synthesis. To prepare the carbon-coated samples, C12A7-550 powder was mixed with polyvinyl alcohol in a 7:3ratio with subsequent calcination in an argon atmosphere at desired temperature. High-temperature treatment of the samples was carried out in a special corundum ampoule. The ampoule was located inside the high-temperature tubular furnace manufactured using Starbar® carbide-silicon heating element with the working temperature interval up to 1500°C. The temperature ramping rate was 4°C/min. Each sample was kept at the final temperature for 6h. X-ray diffraction (XRD) patterns of the samples were recorded using a Bruker D8 diffractometer. Electron paramagnetic resonance (EPR) studies were performed using an ERS-221 EPR spectrometer. EPR spectra were acquired at room temperature. HRTEM images were obtained using a JEM-2010 electron microscope (JEOL Japan) with a lattice-fringe resolution of 0.14nm at accelerating voltage of 200kV. The samples for HRTEM were prepared on a perforated carbon film mounted on a copper grid. The values of SSA calculated by the BET method were determined from the data obtained by low-temperature argon adsorption using an ASAP-2400 instrument. Raman spectra were recorded using a LabRAM HR800 spectrometer from HORIBA Jobin Yvon with a Symphony CCD detector. For spectral excitation the 488 nm line of an Ar<sup>+</sup> laser (35LAP431 from Melles Griot, USA) was used.

## Results and Discussion

### Carbon-coated nanocrystalline TiO<sub>2</sub>

It was found that the carbon coating prevents the sintering of the titania nanoparticles and contributes to the stabilization of their size. In such materials, the particle size of anatase can be stabilized at level of 10-12nm even after heat treatment at 750°C. For instance, in the carbon-coated nanocrystalline TiO<sub>2</sub> (NA-TiO<sub>2</sub>@C), the rutile phase is practically absent whereas the same sample without carbon coating is completely converted to rutile after such procedure Figure 2. When the particle size is small (up to 15 nm), the anatase phase is more thermodynamically stable. Therefore, the rutile phase formation occurs only when the size of the nanoparticles is above this critical value. While the carbon coating prevents the sintering of the nanoparticles at high temperatures, it helps to preserve their size and, consequently, stabilizes the anatase phase.

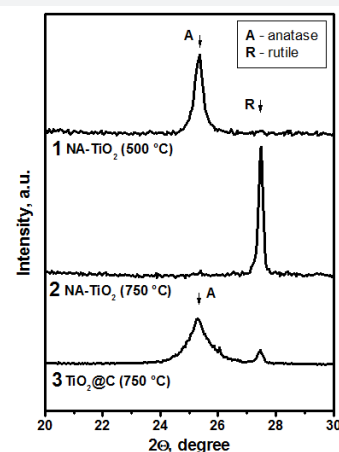


**Figure 2:** XRD patterns of nano crystalline TiO<sub>2</sub> (1,2) and carbon-coated TiO<sub>2</sub>@C(3) after heating at 500 °C (1) and 750°C (2,3).

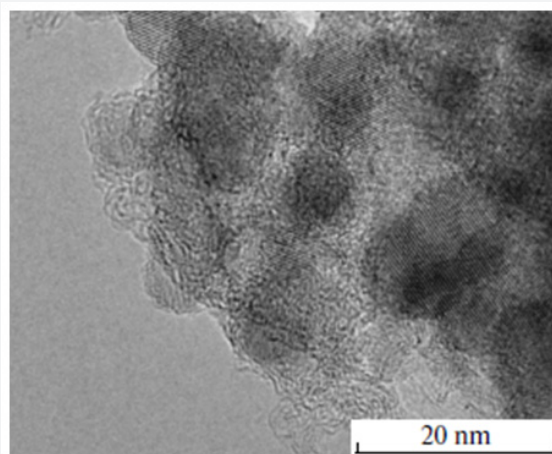


**Figure 3:** HRTEM image of the NA-TiO<sub>2</sub>@C after heating in argon atmosphere at 750°C for 3 hours.

Figure 3 shows a HRTEM image of NA-TiO<sub>2</sub>@C calcined at 750°C. One can see that the size of carbon-coated TiO<sub>2</sub> nanoparticles does not exceed 10-15nm. Meanwhile, the particles of the sample without the coating are 30-40nm in size, and the phase is rutile. The data shown in Figures 2 & 3 clearly demonstrate that the carbon shell stabilizes the size and phase composition of the anatase nanoparticles within it. Figure 4 shows the effect of the carbon coating on the formation of a corundum phase resulting from the high temperature treatment of Al<sub>2</sub>O<sub>3</sub> and Al<sub>2</sub>O<sub>3</sub>@C samples. Complete conversion of the pure  $\gamma$ -Al<sub>2</sub>O<sub>3</sub> precursor to  $\alpha$ -Al<sub>2</sub>O<sub>3</sub> corundum was observed at 1180°C (Figure 3). Meanwhile, practically no corundum was formed in the case of carbon-coated material Al<sub>2</sub>O<sub>3</sub>@C. According to XRD data, only  $\delta$ -Al<sub>2</sub>O<sub>3</sub> phase was observed.

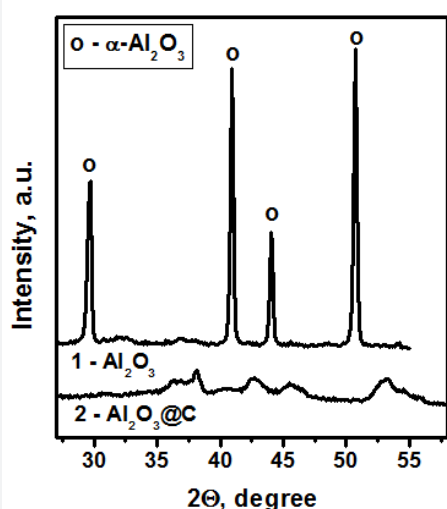


Figure 4: XRD patterns of Al<sub>2</sub>O<sub>3</sub> (1) and Al<sub>2</sub>O<sub>3</sub>@C (2) samples after calcinations at 1180 °C

The size of alumina crystallites was stabilized at 20-25nm. The Al<sub>2</sub>O<sub>3</sub>@C sample could be transformed to corundum only after heat treatment at 1380°C. Most likely, stabilization of the particle size by the carbon shell in Al<sub>2</sub>O<sub>3</sub>@C samples is the main factor preventing their phase transformation to corundum. The growth of the nanoparticles size during the heat treatment naturally results in a loss of their SSA. Changes of the specific surface area of Al<sub>2</sub>O<sub>3</sub> and Al<sub>2</sub>O<sub>3</sub>@C samples after calcination at high temperatures are shown in Figure 5. Fast drop of the surface area at calcination temperatures around 1100°C is clearly observed for pure Al<sub>2</sub>O<sub>3</sub>. These are the temperatures when the corundum phase is formed. Meanwhile, for Al<sub>2</sub>O<sub>3</sub>@C samples relatively high surface area is preserved until the calcination temperature of 1380°C. Raman spectroscopy yields averaged information on the state of the carbon shell in Al<sub>2</sub>O<sub>3</sub>@C samples. As it was recently reported [14], the Raman spectrum of Al<sub>2</sub>O<sub>3</sub>@C sample calcined at 1230°C contains well-developed D at 1350cm<sup>-1</sup>, G at 1587cm<sup>-1</sup>, HWHM G-55cm<sup>-1</sup>, D' at 1615cm<sup>-1</sup> and 2D peaks near 2700cm<sup>-1</sup>. These data indicate the formation of 1-3 monolayer of nanocrystalline graphite [15].

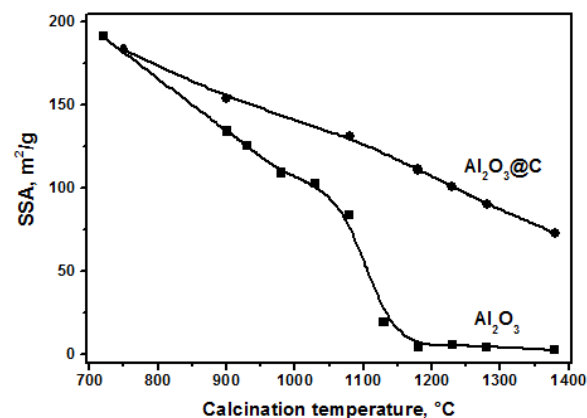


Figure 5: Effect of calcination temperature on SSA of Al<sub>2</sub>O<sub>3</sub> and Al<sub>2</sub>O<sub>3</sub>@C

It should be noted that after removal of the carbon shell by calcination in air, the carbon-coated samples retained clearly visible grey color instead of white color of pure Al<sub>2</sub>O<sub>3</sub> samples. This color appears only for Al<sub>2</sub>O<sub>3</sub>@C samples calcined in an argon flow at relatively high temperature. The Raman spectrum of Al<sub>2</sub>O<sub>3</sub>@C sample calcined in argon at 1230°C and additionally calcined in air at 700°C to burn off the carbon accessible to the gas phase is characterized by the lack of 2D peaks and substantially less intense D and G lines in comparison with the carbon-coated sample. This spectrum can be attributed to nanocrystalline graphite particles encapsulated at places of contact between the Al<sub>2</sub>O<sub>3</sub> nanoparticles, which account for the grey color of the samples.

### Carbon-coated calcium aluminate C12A7

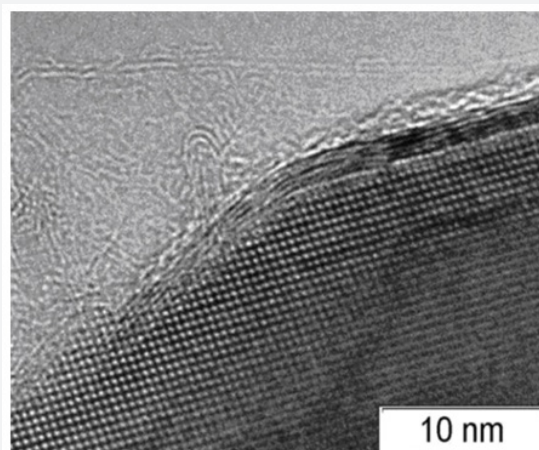
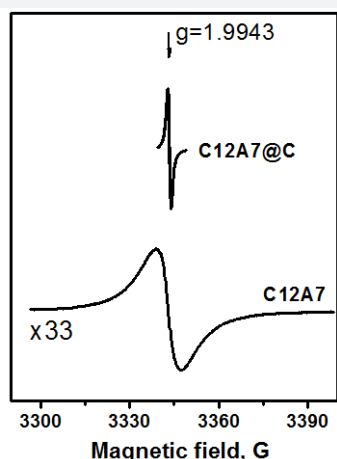


Figure 6: HRTEM images of the carbon shell on the surface of C12A7 micro crystallite after calcinations of C12A7@C sample in argon at 1380°C.

According to the XRD data, the formation of single-phase calcium aluminate C12A7 with mayenite structure occurs starting from 550 °C. This structure is maintained for the samples subjected to treatment in argon at 1450 °C. Intensive

sintering at high temperatures was observed for samples without the carbon coating. The carbon shell prevents sintering, thus allowing synthesizing the samples in a disperse state even at 1450 °C. According to the TEM data, typical dimensions of C12A7 particles inside the carbon shell range from 100 nm to several microns. The carbon shell can have either a disordered structure or dense packing of graphenes into graphite layers (Figure 6). A disordered shell covers the graphite layer additionally shielding the C12A7 crystal surface. Substitution of oxygen anions with  $e^-$  in C12A7@C system, which is the initial stage of the electrode C12A7: $e^-$  formation can be reliably detected by EPR due to appearance of a specific signal at  $g = 1.994$  (Figure 7), which is well-known for bulk C12A7: $e^-$  materials [8,9].



**Figure 7:** EPR spectra of C12A7@C and C12A7 samples calcined at 1380°C.

A similar spectrum with half-width of 8.7G was observed for C12A7 without the carbon coating calcined at 1380°C. Meanwhile, the half-width of the EPR signal for C12A7@C samples was significantly lower and did not exceed 1G. The maximum concentration of paramagnetic sites in C12A7@C materials achieved in our experiments was  $(2 \div 4) \times 10^{19} \text{ g}^{-1}$ , which is close to the literature data for samples synthesized from melts [8,9]. Meanwhile, our C12A7@C: $e^-$  materials possess relatively high surface areas. The SSA of C12A7@C sample was  $24 \text{ m}^2/\text{g}$  after calcination at 1380°C, where as C12A7 without carbon coating after heat treatment at the same temperature was as intered material with the SSA of  $0.1 \text{ m}^2/\text{g}$ . Thereby, the carbon coating prevents agglomeration of core nanoparticles at very high temperatures, and leads to the electrode formation inside the carbon shell. The use of the carbon nanoreactor approach allowed us to obtain the electrode with much higher dispersity if compared with the conventional method starting from the melt.

## Conclusion

The results of the study indicate that preservation of a small particle size is a key factor hindering the phase transformations in the concerned  $\text{TiO}_2$ @C and  $\text{Al}_2\text{O}_3$ @C systems. The presence of the carbon coating inhibits the sintering of the particles and makes it possible to synthesize new materials with the particle size

similar to that of the initial particles of the oxide precursors. The suggested carbon nanoreactor concept can be used for synthesis of nanomaterials of different chemical nature with a wide range of potential use in modern technology. Carbon coating is just one of the ways to form a nanoreactor shell. It is obvious that such a shell will not always be inert and is completely unsuitable for high temperature synthesis in an oxygen environment. The core-shell method can be used to stabilize the size of the oxide core nanoparticles up to temperatures when their reaction with the coating material takes place. In the case of the carbon shell, this is the temperature when the carbothermal reduction of the oxide core begins. A search for other materials that can function as a nanoreactor shell and can make it possible to perform such synthesis in air is of great importance for many practical applications.

## Acknowledgement

Financial support from Russian Science Foundation (project No. 16-13-10168) is acknowledged with gratitude.

## References

- Mishakov IV, Bedilo AF, Richards RM, Chesnokov VV, Volodin AM, et al. (2002) Nanocrystalline MgO as a dehydrohalogenation catalyst. *J Catal* 206(1): 40-48.
- Wang J, Uma S, Klabunde KJ (2004) Visible light photocatalytic activities of transition metal oxide/silica aerogels. *Micropor Mesopor Mater* 75(1-2): 143-147.
- Klabunde KJ, Stark J, Koper O, Mohs C, Park DG, et al. (1996) Nanocrystals as stoichiometric reagents with unique surface chemistry. *J Phys Chem* 100:12142-12153.
- Richards R, LiW F, Decker S, Davidson C, Koper O, et al. (2000) Consolidation of metal oxide Nanocrystals. Reactive pellets with controllable pore structure that represent a new family of porous, inorganic materials. *J Am Chem Soc* 122(20): 4921-4925.
- Wagner GW, Procell LR, Oconnor RJ, Munavalli S, Carnes CL, et al. (2001) Reactions of VX, GB, GD, and HD with nanosize  $\text{Al}_2\text{O}_3$ . Formation of aluminophosphonates. *J Am Chem Soc* 123(8): 1636-1644.
- Mishakov IV, Zaikovskii VI, Heroux DS, Bedilo AF, Chesnokov VV, et al. (2005)  $\text{CF}_2\text{Cl}_2$  decomposition over nanocrystalline MgO: Evidence for long induction periods. *J Phys Chem B* 109(15): 6982-6989.
- Bedilo AF, Shuvarakova EI, Volodin AM, Ilyina EV, Mishakov IV, Vedyagin AA, et al. (2014) Effect of modification with vanadium or carbon on destructive sorption of halocarbons over nanocrystalline MgO: The role of active sites in initiation of the solid-state reaction. *J Phys Chem C* 118(25): 13715-13725.
- Hayashi K, Matsuishi S, Kamiya T, Hirano M, Hosono H, et al. (2002) Light-induced conversion of an insulating refractory oxide into a persistent electronic conductor. *Nature* 419: 462-465.
- Kim SW, Toda Y, Hayashi K, Hirano M, Hosono H, et al. (2006) Synthesis of a room temperature stable  $12\text{CaO} \cdot 7\text{Al}_2\text{O}_3$  electrode from the melt and its application as an electron field emitter. *Chem Mater* 18(7): 1938-1944.
- Kitano M, Inoue Y, Yamazaki Y, Hayashi F, Kanbara S, et al. (2012) Ammonia synthesis using a stable electrode as an electron donor and reversible hydrogen store. *Nature Chem* 4: 934-940.
- Bedilo AF, Sigel MJ, Koper OB, Melgunov MS, Klabunde KJ (2002) Synthesis of carbon-coated MgO nanoparticles. *J Mater Chem* 12: 3599-3604.

12. Heroux DS, Volodin AM, Zaikovskii VI, Chesnokov VV, Bedilo AF, et al. (2004) ESR and HRTEM study of carbon-coated nanocrystalline MgO. J Phys Chem B 108(10): 3140-3144.
13. Volodin AM, Bedilo AF, Mishakov IV, Zaikovskii VI, Vedyagin AA, et al. (2014) Carbon nanoreactor for the synthesis of nanocrystalline high-temperature oxide materials. Nanotechnol Russ 9(11-12): 700-706.
14. Volodin AM, Bedilo AF, Stoyanovskii VO, Zaikovskii VI, Kenzhin RM, et al. (2017) Nanocrystalline carbon coated alumina with enhanced phase stability at high temperatures. RSC Adv 7: 54852-54860.
15. Ferrari AC, Robertson J (2000) Interpretation of Raman spectra of disordered and amorphous carbon. Phys Rev B 61: 14095-14107.



This work is licensed under Creative Commons Attribution 4.0 License  
DOI: [10.19080/JOJMS.2017.03.555617](https://doi.org/10.19080/JOJMS.2017.03.555617)

**Your next submission with Juniper Publishers  
will reach you the below assets**

- Quality Editorial service
- Swift Peer Review
- Reprints availability
- E-prints Service
- Manuscript Podcast for convenient understanding
- Global attainment for your research
- Manuscript accessibility in different formats

**( Pdf, E-pub, Full Text, Audio )**

- Unceasing customer service

**Track the below URL for one-step submission**

<https://juniperpublishers.com/online-submission.php>